IEEE Photonics Journal
An IEEE Photonics Society Publication

Open Access

The Investigation of the Balanced Output Power of Multi-Section Tunable Laser Based On Reconstruction-Equivalent Chirp Technique

Volume 13, Number 1, February 2021

Renjia Guo
Yongbing Zhao
Liangliang Yang
Xiaohua Wang

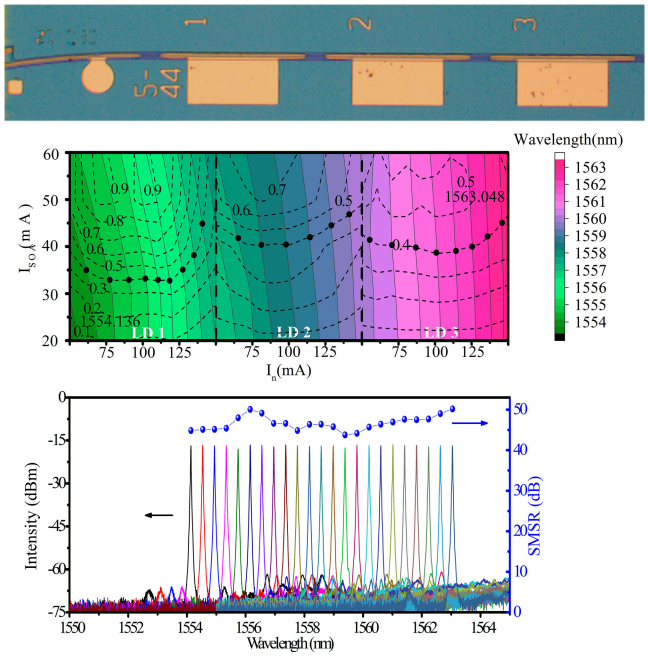

DOI: 10.1109/JPHOT.2020.3044931

The Investigation of the Balanced Output Power of Multi-Section Tunable Laser Based On Reconstruction-Equivalent Chirp Technique

Renjia Guo, Yongbing Zhao, Liangliang Yang, and Xiaohua Wang

School of Physics and Electronic Engineering, Jiangsu Intelligent Optoelectronic Devices and Measurement and Control Engineering Research Center, Yancheng Teachers University, Yancheng 224007, China

DOI:10.1109/JPHOT.2020.3044931

Manuscript received August 29, 2020; revised November 9, 2020; accepted December 11, 2020. Date of publication December 15, 2020; date of current version December 31, 2020. This work was supported in part by the Youth Fund Project of National Natural Science Foundation of China under Grants 61904157 and 61904158, in part by the Emergency Management Project of National Natural Science Foundation of China under Grants 11847161 and 11847166, in part by the General Projects of Natural Science Research in Universities of Jiangsu Province of China under Grants 18KJB510047 and 19KJD140005, and in part by the Cooperation Project of Industry-University-Research of Jiangsu Province of China under Grant BY2020630 and BY2020613. Corresponding author: Renjia Guo (e-mail: guorj@yctu.edu.cn).

Abstract: A method to get balanced output power of a current-controlled in-line semiconductor laser based on REC technique is investigated. By mapping the contour lines of the P-I contour diagram of this in-line tunable laser into the wavelength-current contour map, the maximum output power and the tuning curve is obtained. Numerical studies are carried on under linear and quadratic relations, as well as an experiment measurement. Results shows it's a feasible method to find the maximum output power and obtain working currents for the current-controlled in-line semiconductor lasers.

Index Terms: Diode laser arrays, distributed feedback lasers, tunable lasers.

1. Introduction

Tunable lasers can be used widely in future functional optical systems such as wavelength division multiplexing (WDM) systems and reconfigurable optical add-drop multiplexers (RODAMs). [1] While various methods have already been proposed to achieve semiconductor wavelength tunable laser devices [2]–[6], the cost is now a major factor decides which device can be widely used in commercial market. In-line multi-wavelength laser array is also a device proposed to realize a tunable laser [7], [8], with reconstruction-equivalent chirp (REC) technique, the fabrication of such multi-wavelength array can be simplified and the cost can be lowered [9]–[12]. Recently, an in-line tunable laser employs only current tuning has been demonstrated [13]. Via changing the driving current and switching laser, continues tuning range of $\sim$12 nm is achieved, provides a potential approach of the very low cost tunable laser. Moreover, the wavelength switching time is several tens of milliseconds, which is also very important for the ultra-wideband applications. However, changing the driving current will lead a variation of output power, and it is not favored in communication systems. Thus a power adjusting component is also needed for this current tuned

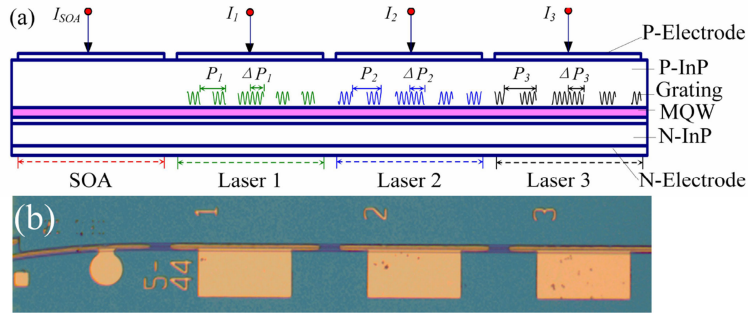

Fig. 1. (a) Schematic and (b) microscope image of a multi-electrodes DFB tunable semiconductor laser with SOA.

laser, and monolithic integrated semiconductor optical amplifier (SOA) is a common choice. In real devices, the integrated SOA itself also has a heating effect, which will change the output wavelength while adjusting the output power. Till now no attention has been paid on the characteristic of such current-controlled in-line semiconductor laser and its current tuning algorithm. So in this work we further studied the control algorithm of the current applied on SOA and working laser based on our REC in-line tunable lasers. The applied driving currents are obtained by two contour diagrams, from which maximum output power can also be predicted and a tuning curve can be obtained for determining the driving current of the laser and SOA. The results provide an important characterizing method and control algorithm for such in-line, current-controlled semiconductor laser.

2. Method and Numerical Studies

The schematic and the microscope image of a multi-electrodes distributed feedback (DFB) tunable semiconductor laser with SOA are shown in Fig. 1. The designed inter spacing between adjacent lasers is 3.2 nm. Both front and rear end facets are anti-reflection coated, and the waveguide of the front end is tilted (10°) to further reduce the reflection. The minimum reflection can be found at the tilt angle of 10° by simulating the fundamental TE mode profile of the slab waveguide. The power reflection coefficient is obtained from means of the mode width parameter with the Fresnel reflection coefficient. [14] In such in-line laser array, when the working laser is not the closest one to the output facet, the lasers in front of it needs to be applied a current to compensate the propagation loss and such current is called transparency current. In our test, the transparency current of front laser keeps 25 mA. The common tuning method is relative simple, which is, changing the driving current of the working laser to change the output wavelength, and meanwhile tuning the driving current of the SOA reversely to balance the output power. A major characteristic value of this tunable laser is the maximum output power that can be obtained in continues wavelength tuning. For larger output power needs a larger driving current, the available tuning range will be reduced by the smaller current tuning range. So it is necessary to find out a proper output power.

Firstly, an ideal condition is considered, and in this circumstance the power and wavelength variation is assumed to change linear with injection current. In the tuning, only the driving current of the working laser and the SOA are adjusted, so the output power P and the wavelength λ can be written as a function of the driving current I_{SOA} and I_n, which refer the current applied on SOA and the nth laser respectively:

$$\begin{pmatrix} P \\ \lambda \end{pmatrix} = \begin{pmatrix} a & b \\ c & d \end{pmatrix} \begin{pmatrix} I_{SOA} \\ I_n \end{pmatrix} + \begin{pmatrix} P_0 \\ \lambda_0 \end{pmatrix} \quad (n = 1, 2, 3) \tag{1}$$

In equation (1), a, b, c and d are the coefficient in the linear assumption. Usually, a $>$ b, c $<$ d, for the current directly applied on the working laser will cause a more effective changing in the output power and wavelength than that applied on SOA. According to our previous test, the coefficients a,

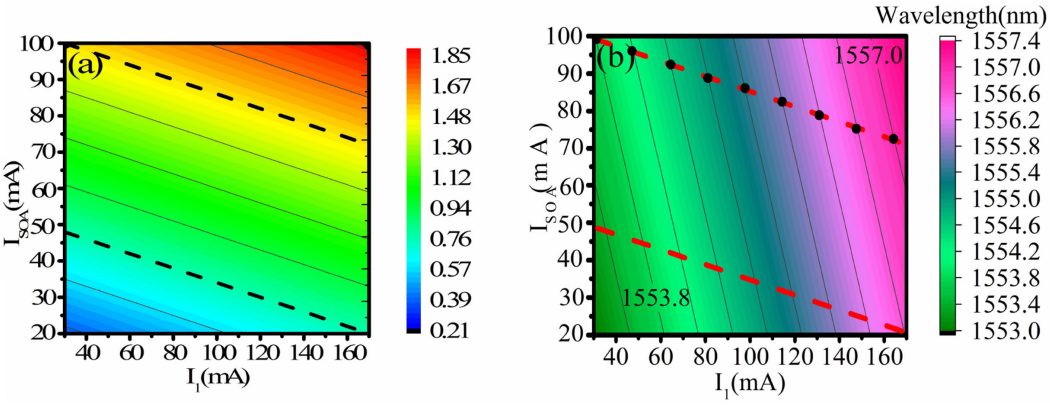

Fig. 2. (a) Output power and (b) wavelength with mapped power contour of LD1of tunable laser with different current in linear situation.

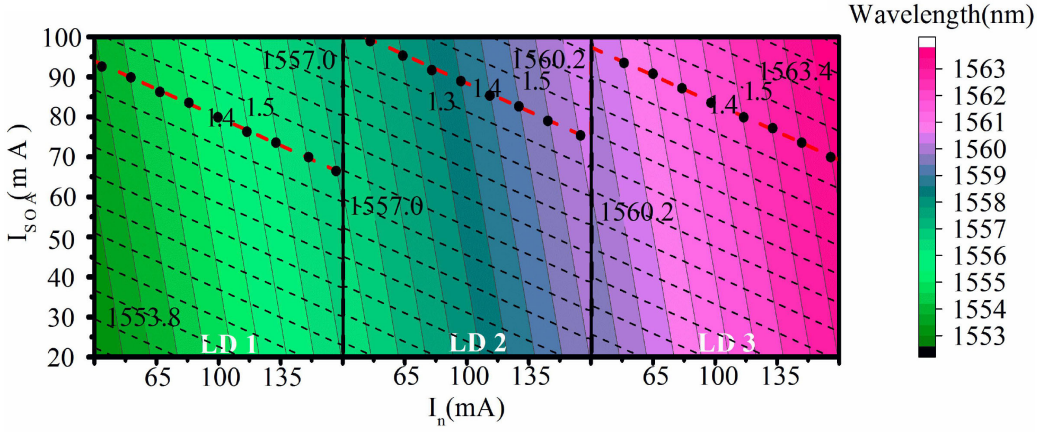

Fig. 3. Linear wavelength-current contour map of all three in-line lasers, mapped with linear P-I contour lines.

b, c and d are taking the value of 0.014 mW/mA, 0.0028 mW/mA, 0.01 nm/mA, and 0.026 nm/mA, respectively. Then, when the current tuning range of SOA is 20-100 mA, and that of working laser is 30–170 mA, the output power and wavelength within the tunable range of LD 1 are shown in Fig. 2.

In this linear situation, the maximum wavelength range could get with I_{SOA} from 50 to 100 mA and I_1 from 30 to 170 mA as the area between two dash lines (Fig. 2). The highest power lever is about 1.48 mW (upper dash line in Fig. 2(a)) with $I_{SOA} = 100$ mA and $I_1 = 30$ mA. In this case, the wavelength tunable range is 3.2 nm from 1553.8 to 1557.0 nm, which matches lasers' inter spacing 3.2 nm, and contains 9 channels for LD1 with 50 GHz channel spacing (Fig. 2(b)). For an in-line array with three lasers, the tuning curve is shown in Fig. 3. The maximum available output power is the up-most P-I line that can go through all wavelengths, which are represented by different colors in the contour map. Then, the value of maximum output power obtained here is about 1.4 mW.

In practical device, large laser power and high temperature will cause a saturation of the P-I relation. The optical output power of the proposed laser versus the injection currents of the LD1 and the SOA is measured for our tunable laser, and is shown in Fig. 4. It is found that for small-injection currents less than 90 mA, the output power increased. Whereas for large-injection currents above 100 mA, the output power decreased. In other words, the output power is saturated and even drops

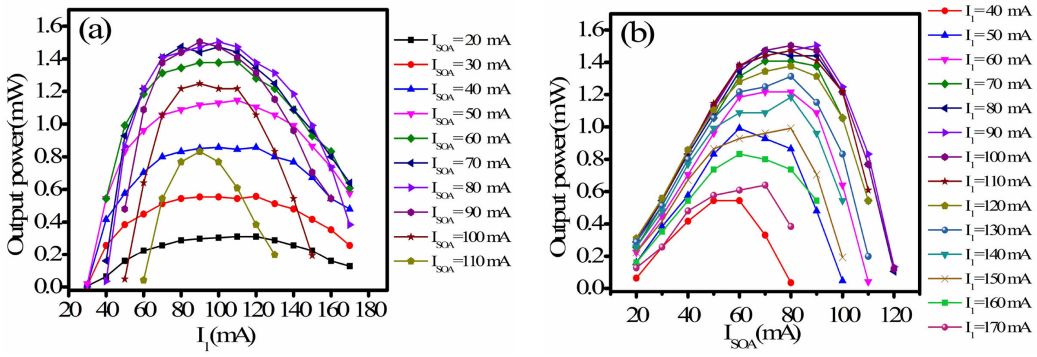

Fig. 4. Measured P-I relation of current-tuned in-line semiconductor laser (a) P-I curve of LD1 under different I_{SOA} value; (b) P-I curve of SOA under different I_1 value.

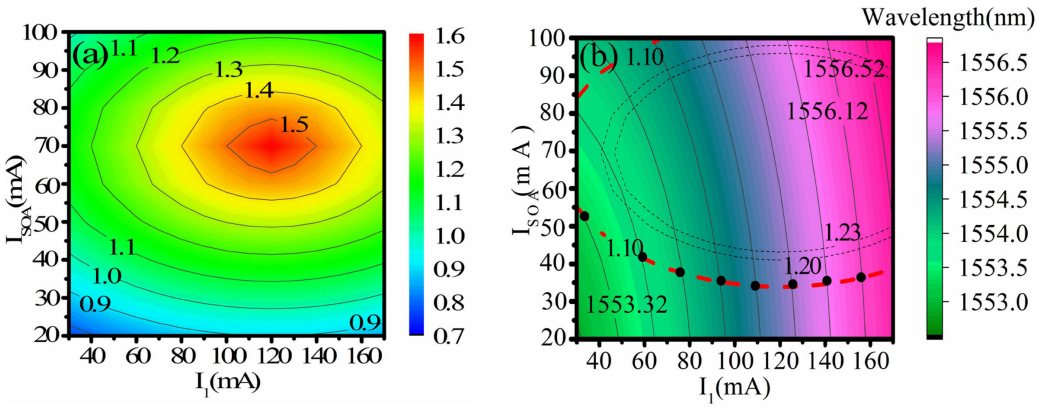

Fig. 5. (a) Output power and (b) wavelength with mapped power contour of LD1 of tunable laser with different current in quadratic simulation.

at high-injected current. A maximum output power of about 1.5 mW is achieved under I_1 and I_{SOA}. both of 90 mA. This is due to the gain saturation and thermal effect in the SOA. Furthermore, the in-line structure reduces the thermal conductivity to enlarge the heating effect of the LD1 under the high-driving current of the SOA. The P-I curve will saturate and even decrease more rapidly under larger driving current of the SOA. We note that this faster degradation of the P-I curve of $I_{SOA} =$ 110 mA is expected to be fundamentally different from that of the others. So the curve of $I_{SOA} =$ 110 mA in Fig. 4(a) is pretty abnoral from the others. In this situation, linear relation can't give a proper result. Because of the saturation and power decreasing caused by over-heat, the P-I curve is usually appears like a quadratic curve.

So further discussing using a quadratic relation to describing the relations in output power P, wavelength λ, the current of SOA I_{SOA} and the current of the working laser I_n. The relation is written as:

$$\begin{pmatrix} P \\ \lambda \end{pmatrix} = \begin{pmatrix} a & b \\ c & d \end{pmatrix} \begin{pmatrix} I_{SOA}{}^2 \\ I_n{}^2 \end{pmatrix} + \begin{pmatrix} e & f \\ g & h \end{pmatrix} \begin{pmatrix} I_{SOA} \\ I_n \end{pmatrix} + \begin{pmatrix} P_0 \\ \lambda_0 \end{pmatrix} \quad (n = 1, 2, 3) \tag{2}$$

Then the output power and wavelength within the tunable range of LD1 are shown in Fig. 5.

Obviously, the quadratic relation produces eclipse-shaped contour lines. The tuning curve can be obtained by mapping the contour lines in Fig 5(a) into the Fig 5(b), and then the corresponding points along the same mapped line will have the same output power, while the output wavelengths are different along it. So the tuning curve can be determined. These figures also show that in a quadratic relation, the wavelength tunable range decreases with the increasing of the output power

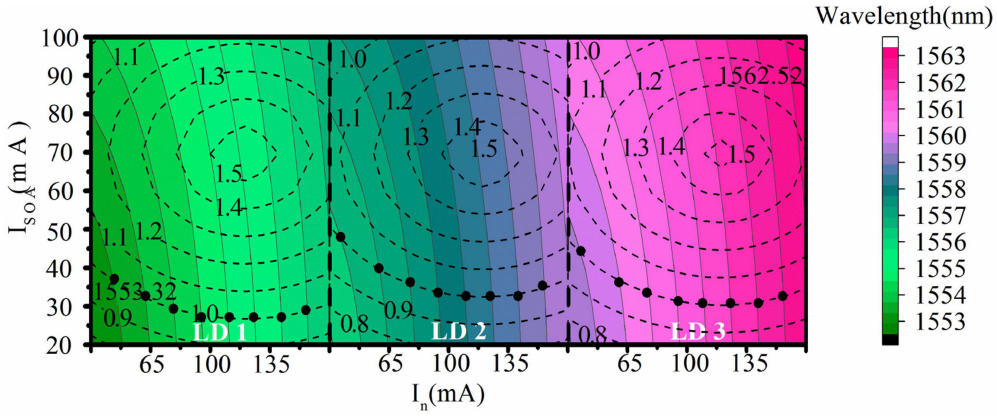

Fig. 6. The total mapped contour of output power and wavelength of in-line tunable laser in quadratic simulation.

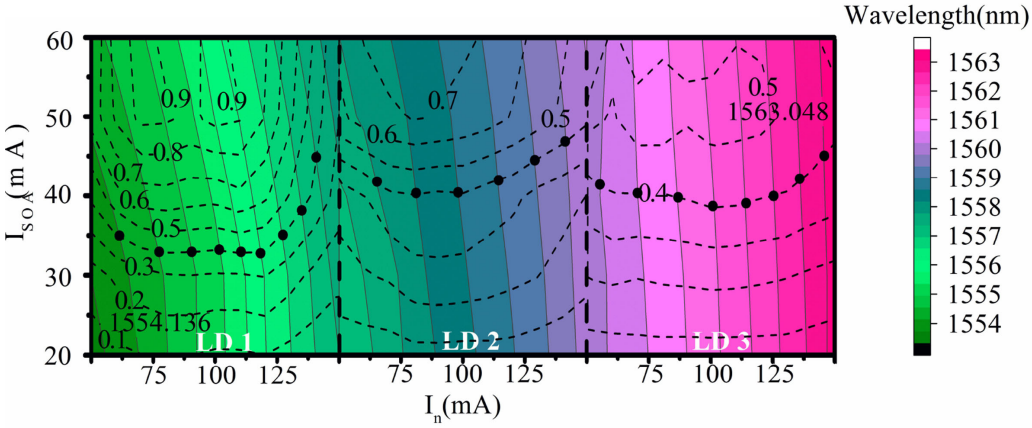

Fig. 7. The total mapped contour of output power and wavelength of in-line tunable laser in the experiment.

more rapidly. So there is a smaller maximum output power for continues wavelength tuning than linear assumption, and beyond this power value, the current tuning cannot cover all wavelength in the tuning range.

To get the maximum output power for all three in-line lasers, the wavelength contour maps of all three lasers are put together as shown in Fig. 6. The contour lines that represent different power values are also mapped into them. The maximum power that covers all available wavelength is the maximum power of the tunable laser, and in Fig. 6 it is found to be about 1.0 mW (marked by black round dots in Fig. 6). The output power larger than it cannot cover all the wavelengths in the whole tunable range. The proper driving currents for any wavelength channel are also obtained, and the point corresponding to the applied current should be on the contour line represents the maximum power value.

3. Experiment Results

In experiments, the contour maps are obtained by separate P-I measurements and wavelength-current measurements, and the diagram of one real in-line tunable chip is shown in Fig. 7.

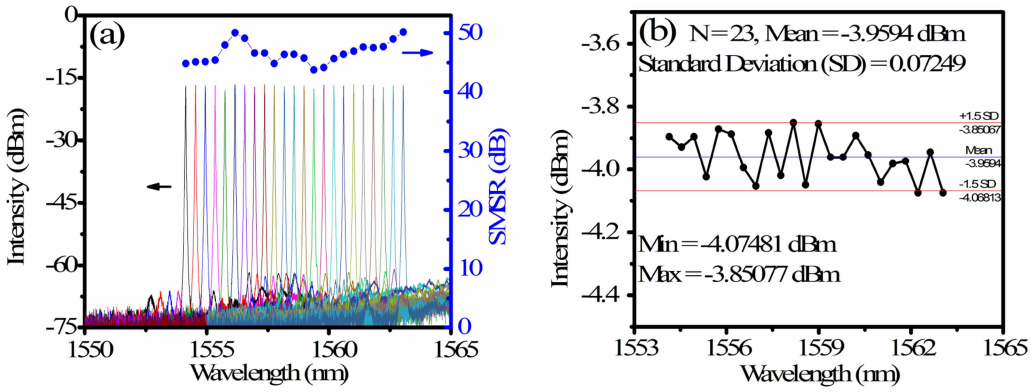

Fig. 8. Measured (a) spectra with SMSRs and (b) output power of 23 channels with 50 GHz channel spacing of proposed tunable laser.

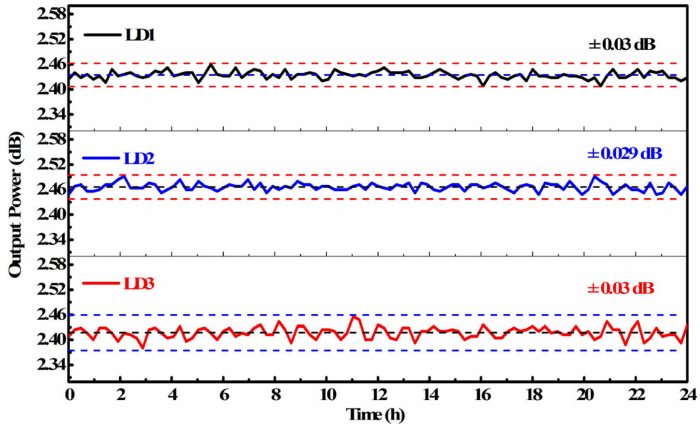

Fig. 9. Stability of the output power of the proposed tunable laser within 24 hours.

From Fig. 6, the numerical contours of all three in-line lasers are carried out under the same P-I and wavelength-current condition to study the balanced output power with the maximum power value. So the wavelength and output power spacing is the same throughout all three in-line lasers for the idealized model in the simulation. The numerical contours are quadratic. But the wavelength and output power spacing of the experimental contour in Fig. 7 is different from each other. The wavelength contour of LD2 and LD3 are more vertical than that of the LD1 in the experimental contour, because the wavelength of LD2 and LD3 are affected less by the heat generated in SOA part than that of LD1. The output power contour of LD3 is sparsest of those of all three in-line lasers. This is because of the most absorptive dissipation of LD3 to throughout all the waveguide of in-line tunable laser than those of LD1 and LD2. The maximum output power and tuning curve still can be obtain form the contour maps, which is marked by the black dots in the figure. These results indicate that the real power and wavelength contours are neither linear nor quadratic.

This wavelength tunable range contains 23 channels with 50 GHz channel spacing from 1554.136 to 1563.048 nm (192.9–191.8 THz) for the current-controlled in-line semiconductor laser, and the maximum power is available for all channels is about 0.4 mW here. All channels are found out from the diagram and the corresponding spectrums, side-mode suppressing ratios (SMSRs) and the balanced output power are shown in Fig. 8. The output power from the proposed laser was connected to an ILX Lightwave OMM-6810B power meter. It shows how the laser output power will vary over the course of 24 hours in Fig. 9. Long term power stabilities of LD1, LD2 and LD3 are within $\pm$ 0.03 dB, $\pm$ 0.029 dB and $\pm$ 0.03 dB, respectively.

4. Conclusion

By mapping the contour lines of the P-I contour diagram of this in-line tunable laser into the wavelength-current contour map, the maximum output power and the tuning curve are obtained. Numerical studies are carried on under linear and quadratic assumptions. In linear situation, the tuning curve is simple along a slope line and in quadratic situation it is along the arc shaped curve. Maximum available output power is obtained from up-most P-I contour line that can go through each wavelength-current contour diagram, from the very left to the very right. Experiments are carried on a real in-line three laser array and results show it's a feasible method to find the maximum output power and obtain working currents for the current-controlled in-line semiconductor lasers.

Acknowledgment

The authors would like to thank Prof. Xiangfei Chen and Dr. Jun Lu for valuable discussion of revising the manuscript.

References

[1] W. Bogaerts *et al.*, "Programmable photonic circuits," *Nature*, vol. 586, pp. 207–216, 2020, Art. no. 7828.
[2] S. Yamaoka *et al.*, "Directly modulated membrane lasers with 108 GHz bandwidth on a high-thermal-conductivity silicon carbide substrate," *Nat. Photon.*, vol. 15, pp. 28–35, 2021.
[3] M. Kuznetsov, P. Verlangieri, A. Dentai, C. Joyner, and C. Burrus, "Widely tunable (45 nm, 5.6 THz) multi-quantum-well three-branch Y3-lasers for WDM networks," *IEEE Photon. Technol. Lett.*, vol. 5, no. 8, pp. 879–882, 1993.
[4] A. Ward *et al.*, "Widely tunable DS-DBR laser with monolithically integrated SOA: Design and performance," *IEEE J. Sel. Topics. Quantum Electron.*, vol. 11, no. 1, pp. 149–156, 2005.
[5] A. Sivananthan *et al.*, "Integrated linewidth reduction of a tunable SG-DBR laser," in *Proc. Conf. Lasers Electro-Opt. (CLEO)*, 2013, pp. CTu1L.2.
[6] T. Kanai, N. Nunoya, T. Yamanaka, R. Iga, M. Shimokozono, and H. Ishii, "High-accuracy, sub-μs wavelength switching with thermal drift suppression in tunable distributed amplification (TDA-) DFB laser array," in *Proc. Opt. Fiber Commun. Conf.*, 2013, pp. OTh3I.2.
[7] D. McIntosh *et al.*, "Continuously tunable laser based on multiple-section DFB laser technology for 1.25 gbps WDM-PON applications," in *Proc. Conf. Lasers Electro-Opt.*, 2015, pp. SF1I.3.
[8] L. Li, S. Tang, J. Lu, Y. Shi, B. Cao, and X. Chen, "Study of cascaded tunable DFB semiconductor laser with wide tuning range and high single mode yield based on equivalent phase shift technique," *Opt. Commun.*, vol. 352, pp. 70–76, 2015.
[9] J. Li, S. Tang, J. Wang, Y. Liu, X. Chen, and J. Cheng, "An eight-wavelength BH DFB laser array with equivalent phase shifts for WDM systems," *IEEE Photon. Technol. Lett.*, vol. 26, no. 16, pp. 1593–1596, 2014.
[10] Y. Shi *et al.*, "High channel count and high precision channel spacing multi-wavelength laser array for future PICs," *Sci. Rep.*, vol. 4, 2014, Art. no. 7377.
[11] Y. Shi *et al.*, "Study of the multiwavelength DFB semiconductor laser array based on the reconstruction-equivalent-chirp technique," *J. Lightw. Technol.*, vol. 31, no. 20, pp. 3243–3250, 2013.
[12] J. Lu, S. Liu, Q. Tang, H. Xu, Y. Chen, and X. Chen, "Multi-wavelength distributed feedback laser array with very high wavelength-spacing precision," *Opt. Lett.*, vol. 40, no. 22, pp. 5136–5139, 2015.
[13] R. Guo *et al.*, "Multi-section DFB tunable laser based on REC technique and tuning by injection current," *IEEE Photon. J.*, vol. 8, no. 4, 2016, Art. no. 1503007.
[14] D. Marcuse, "Reflection loss of laser mode from tilted end mirror," *J. Lightw. Technol.*, vol. 7, no. 2, pp. 336–339, 1989.